

# Islet-Specific Expression of CXCL10 Causes Spontaneous Islet Infiltration and Accelerates Diabetes Development<sup>1</sup>

Antje Rhode,\* Mary E. Pauza,<sup>†</sup> Ana Maria Barral,\* Evelyn Rodrigo,\* Michael B. A. Oldstone,<sup>‡</sup> Matthias G. von Herrath,\* and Urs Christen<sup>2\*§</sup>

**During inflammation, chemokines are conductors of lymphocyte trafficking. The chemokine CXCL10 is expressed early after virus infection. In a virus-induced mouse model for type 1 diabetes, CXCL10 blockade abrogated disease by interfering with trafficking of autoaggressive lymphocytes to the pancreas. We have generated transgenic rat insulin promotor (RIP)-CXCL10 mice expressing CXCL10 in the  $\beta$  cells of the islets of Langerhans to evaluate how bystander inflammation influences autoimmunity. RIP-CXCL10 mice have islet infiltrations by mononuclear cells and limited impairment of  $\beta$  cell function, but not spontaneous diabetes. RIP-CXCL10 mice crossed to RIP-nucleoprotein (NP) mice expressing the NP of the lymphocytic choriomeningitis virus in the  $\beta$  cells had massively accelerated type 1 diabetes after lymphocytic choriomeningitis virus infection. Mechanistically, we found a drastic increase in NP-specific, autoaggressive CD8 T cells in the pancreas after infection. In situ staining with H-2D<sup>b</sup>(NP<sub>396</sub>) tetramers revealed islet infiltration by NP-specific CD8 T cells in RIP-NP-CXCL10 mice early after infection. Our results indicate that CXCL10 expression accelerates the autoimmune process by enhancing the migration of Ag-specific lymphocytes to their target site. *The Journal of Immunology*, 2005, 175: 3516–3524.**

Inflammation is initially orchestrated by chemokines and cytokines that form an integral part of the innate immune defense against pathogens such as viruses. The ligands of the CXCR3 CXCL9 (monokine induced by IFN- $\gamma$ ), CXCL10 (IFN-inducible protein of 10 kDa (IP-10)<sup>3</sup>), and CXCL11 (IFN-inducible T cell  $\alpha$  chemoattractant) play an important role in autoimmune disease (1–3). CXCR3 chemokine ligands are mainly expressed by keratinocytes, macrophages, fibroblasts, and endothelial cells upon stimulation with IFN- $\gamma$  or TNF- $\alpha$  (4, 5), but are also generated by activated T cell hybridomas, normal T cells, and thymocytes (6). CXCL10 was suggested to function as a sentinel molecule in host defense against viruses (7) and is generated at an early phase of infection with a wide variety of viruses, such as HIV, adenovirus, lymphocytic choriomeningitis virus (LCMV), Theiler's virus, and mouse hepatitis virus (8–12). Furthermore, CXCR3 chemokines are essential in the host defense against for-

eign pathogens by promoting local inflammation. Blockade of CXCL10 disturbed the control of parasite propagation after *Toxoplasma gondii* infection by abrogating T cell migration into tissues and impairing Ag-specific T cell function, resulting in amplified tissue parasite burden and increased mortality (13). Furthermore, transgenic CXCL10 expression in keratinocytes resulted in delayed wound healing and disorganized neovascularization due to a more intense inflammatory phase (14).

CXCR3, the only cellular receptor for CXCL9, CXCL10, and CXCL11 identified to date, is predominantly found on activated Th1-type T cells (15, 16). Thus, CXCR3 chemokine ligands direct the antiviral defense toward the more aggressive type 1 T cell domination and act as bystander effectors that unspecifically activate T cells (including autoreactive T cells). Thus, CXCR3 chemokine ligands can drive an autoaggressive immune response that may result in autoimmune disease. Indeed, recent data from our laboratory suggest that among CXCR3 chemokines, CXCL10 plays a unique and important role in imprinting a pattern for the subsequent development of autoimmunity (2). Briefly, neutralization of CXCL10, but not CXCL9, abrogates autoimmune disease in the rat insulin promotor (RIP)-LCMV mouse model for type 1 diabetes (T1D) by impeding the expansion of Ag-specific CD8 T cells in the periphery and hindering their subsequent migration into the pancreatic target organ (2). Similarly, CXCL10 neutralization was shown to decrease the incidence of T1D in NOD mice after cyclophosphamide administration (17). In contrast, CXCL10 can abrogate diabetes when expressed outside the pancreas. We found that infection with a virus that predominantly expands in the pancreatic draining lymph node (PDLN), at a time when the autoaggressive immune response is already ongoing, abrogates T1D in both the RIP-LCMV and the NOD mouse (18). Apparently, autoaggressive cells migrated from the islets to the PDLN attracted by high CXCL10 concentrations. Once they entered the highly inflamed PDLN, the cells died by apoptosis (18).

To evaluate how enhanced expression of a unique chemokine at the target site for autoimmunity influences the outcome of disease, we generated transgenic mice that express CXCL10 specifically in

\*Immune Regulation Laboratory, Department of Developmental Immunology, La Jolla Institute for Allergy and Immunology, San Diego, CA 92121; <sup>†</sup>Department of Medical Microbiology, Immunology and Cell Biology, Southern Illinois University School of Medicine, Springfield, IL 62702; and <sup>‡</sup>Division of Virology, Department of Neuropharmacology and Department of Infectology, The Scripps Research Institute, La Jolla, CA 92037; and <sup>§</sup>Pharmazentrum, Johann Wolfgang Goethe University, Frankfurt-am-Main, Germany

Received for publication March 11, 2005. Accepted for publication July 13, 2005.

The costs of publication of this article were defrayed in part by the payment of page charges. This article must therefore be hereby marked *advertisement* in accordance with 18 U.S.C. Section 1734 solely to indicate this fact.

<sup>1</sup> U.C. was supported by National Institutes of Health Grant DK66346 and was a recipient of a career development award from the American Liver Foundation. M.G.v.H. was supported by National Institutes of Health Grants AI44451, DK51091, and AI51973. M.B.A.O. was supported by National Institutes of Health Grant DK58541. This is publication 675 of the Department of Developmental Immunology, La Jolla Institute for Allergy and Immunology.

<sup>2</sup> Address correspondence and reprint requests to Dr. Urs Christen, Pharmazentrum, Johann Wolfgang Goethe University, Theodor-Stern Kai 7, D-60590 Frankfurt-am-Main, Germany. E-mail address: christen@med.uni-frankfurt.de

<sup>3</sup> Abbreviations used in this paper: IP-10, IFN- $\gamma$ -inducible protein of 10 kDa; GP, glycoprotein; ICCS, intracellular cytokine assay; LCMV, lymphocytic choriomeningitis virus; NGS, normal goat serum; NP, nucleoprotein; PDLN, pancreatic draining lymph node; RIP, rat insulin promotor; RPA, RNase protection assay; T1D, type 1 diabetes.

the  $\beta$  cells of pancreatic islets of Langerhans. We crossed such RIP-CXCL10 mice to RIP-NP or RIP-GP mice that express the LCMV nucleoprotein (NP) or glycoprotein (GP), respectively (19, 20). In RIP-LCMV mice, the expression of either target Ag per se does not lead to  $\beta$  cell dysfunction, islet cell infiltration, hyperglycemia, or spontaneous activation of autoreactive (anti-LCMV) lymphocytes. However, infection with LCMV results in T1D in >95% of RIP-LCMV mice (20). The onset of T1D in RIP-LCMV mice varies between the individual transgenic lines ranging from 2 wk (RIP-GP line) to 1–6 mo (RIP-NP line) and is dependent on whether the target Ag is expressed in the thymus (RIP-NP line) or not (RIP-GP line) (20). Several lines of evidence indicated that in RIP-NP mice, anti-self (viral) CTL are of low affinity, and CD4 T cells are essential for generation of anti-self (viral) CD8 lymphocyte-mediated T1D (20). An advantage of the RIP-LCMV system over other established models for T1D is the presence of extensively characterized target Ags that allow precise analysis of the immune response against target Ags, including the tracking of LCMV-specific CD8 T cells by in situ MHC class I peptide staining of quick-frozen tissue sections (21).

We report that transgenic mice expressing CXCL10 specifically in the  $\beta$  cells exhibit spontaneous peri-insular and intrinsular infiltration by CD8 and CD4 T cells, but do not develop spontaneous

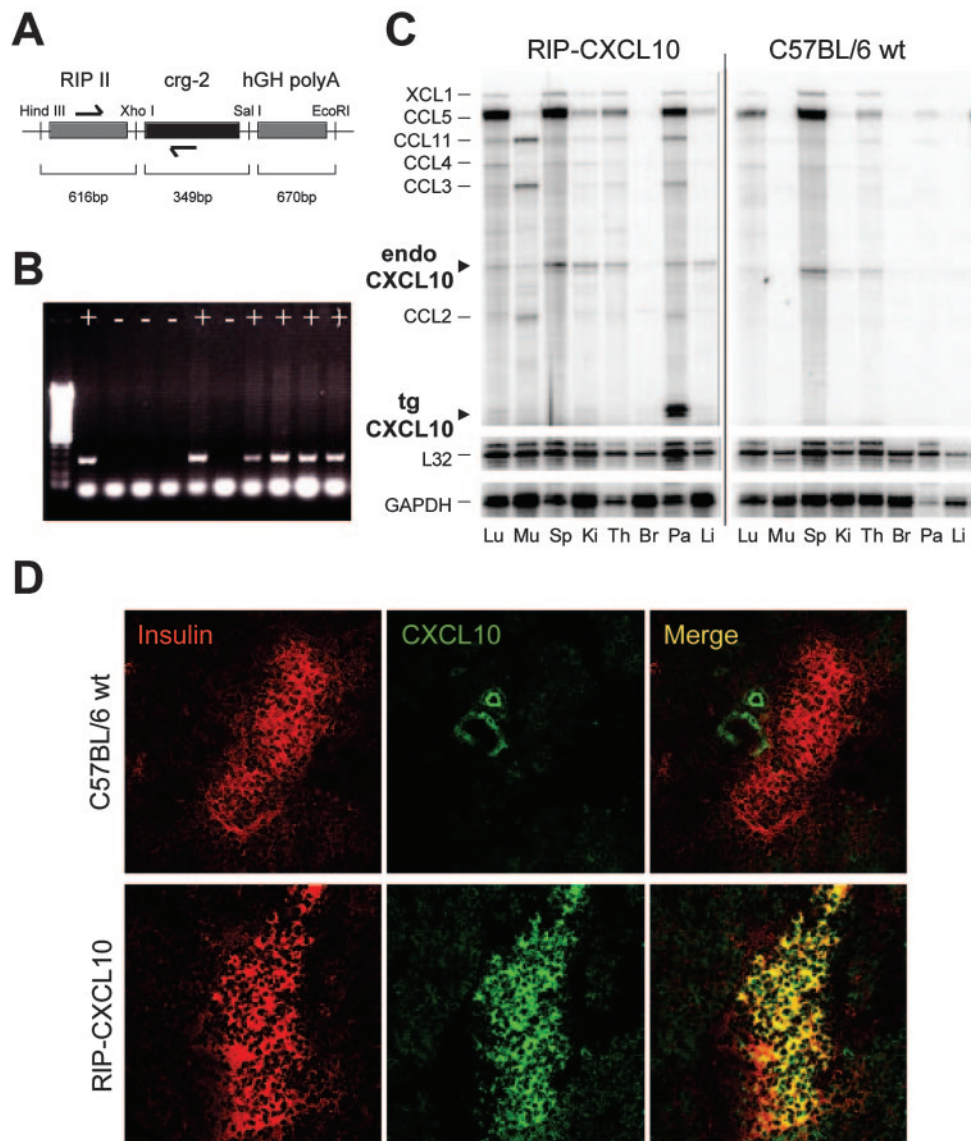
diabetes, indicating that Ag-nonspecific (bystander) activation is not sufficient to induce autoimmunity. However, when crossed with RIP-LCMV mice and infected with LCMV, T1D is greatly accelerated. Within 4 wk of LCMV infection, autoaggressive Ag-specific CD8 T cells were found in islets of diabetic RIP-NP-CXCL10 double-transgenic mice, but not in single transgenic control mice. We conclude from our studies that CXCL10 accelerates the autoimmune process by enhancing the attraction of Ag-specific lymphocytes to their target site.

## Materials and Methods

### Transgenic mouse lines

RIP-CXCL10 transgenic mice were generated by microinjection of a construct containing mouse CXCL10 cDNA. Briefly, CXCL10 was amplified from LPS-stimulated B10.D2 fibroblasts in a standard RT-PCR using *Pfu* DNA polymerase (Promega). After sequence verification, CXCL10 was subcloned into a modified pGEM11Zf<sup>-</sup> vector containing the rat insulin II promoter and human growth hormone poly(A) sequences. An *EcoRI/HindIII* fragment containing the RIP-CXCL10-hGHpoly(A) construct (Fig. 1A) was injected into pronuclei of fertilized C57BL/6J mouse eggs, then eggs were implanted into the oviduct of pseudopregnant recipient mice at the Scripps Transgenic and Embryonic Stem Cell core facility. Offspring were screened for transgene insertion by PCR (Fig. 2B) using the following primers: RIP sense, 5'-GAA-ACC-ATC-AGC-AAG-CAG-GT; and CXCL10 antisense, 5'-GTG-GCA-ATG-ATC-TCA-ACA-CG. Generation

**FIGURE 1.** RIP-CXCL10 mice express CXCL10 specifically in the islets of Langerhans. **A**, Mouse CXCL10 (*crg-2*) cDNA was generated from a C57BL/10 fibroblast cell line (B10.D2) and cloned behind RIP into a pGEM112f<sup>-</sup> plasmid. An *EcoRI/HindIII* fragment, 1619 bp in length, was used for injection into C57BL/6 oocytes. **B**, Typical PCR screening assay for the presence of transgenic DNA construct, designed to distinguish transgenic from wild-type genes using oligonucleotides that hybridize in both the RIP and CXCL10 gene regions (see arrows in A). **C**, RPA of total RNA isolated from various organs, including lung (Lu), skeletal muscle (Mu), spleen (Sp), kidney (Ki), thymus (Th), brain (Br), pancreas (Pa), and liver (Li), using the RiboQuant multiprobe set mCK-5 (BD Pharmingen). Due to a polymorphism in the CXCL10 gene, the use of the mCK-5 set allows us to distinguish between endogenous (C57BL/6) CXCL10 and transgenic (C57BL/10) CXCL10. Note that transgenic CXCL10 is exclusively expressed in the pancreas. **D**, Tissue sections taken from pancreata of 4-wk-old RIP-CXCL10 mice were analyzed for CXCL10 protein expression (green) in the islets of Langerhans. Note that CXCL10 expression colocalizes with the expression pattern of insulin (red), indicating  $\beta$  cell-specific expression of CXCL10.



and screening by PCR of H-2<sup>b</sup> RIP-GP and H-2<sup>b</sup> RIP-LCNV-NP transgenic mice were previously described (19, 20). These mice have been backcrossed to a C57BL/6J background for >10 years. RIP-NP-CXCL10 and RIP-GP-CXCL10 double-transgenic mouse lines were generated by crossing RIP-CXCL10 single-transgenic mice to either RIP-NP or RIP-GP single-transgenic lines, respectively. These studies were approved by the La Jolla Institute of Allergy and Immunology animal care committee.

### Virus

LCMV Armstrong clone 53b (LCMV-Arm) were plaque-purified three times on Vero cells, and stocks were prepared by a single passage on BHK-21 cells. Six- to 10-wk-old mice were infected with a single dose of 10<sup>5</sup> PFU i.p. (20).

### Blood glucose values

Blood samples were obtained from the retro-orbital plexus or from the tail vein. Blood glucose was monitored with a OneTouch Ultra at weekly intervals. Diabetes was defined as blood glucose values >300 mg/dl (22).

### Glucose tolerance assay

Mice were fasted for 12–16 h and then received a single i.p. injection of 1.5 mg/g body weight glucose (Sigma-Aldrich). Blood glucose was measured immediately before injection and then at 10, 20, 30, 40, 60, 120, and 240 min after injection.

### RNase protection assay (RPA)

Total RNA was isolated from whole pancreas homogenates using Tri-Reagent (Molecular Research Center). RNA was extracted with chloroform, followed by isopropanol precipitation and washing with ethanol. Twenty micrograms of total pancreatic RNA was used for hybridization with a [<sup>32</sup>P]UTP-labeled multitemplate set containing specific probes for various chemokines (RiboQuant, mCK-5; BD Pharmingen). The RPA was conducted according to the manufacturer's guidelines. The resulting analytical acrylamide gel was scanned using a Storm-860 PhosphorImaging System (Molecular Dynamics), and the intensities of bands corresponding to protected mRNA were quantified using ImageQuant image analysis software (Molecular Dynamics) and L32 as a reference gene.

### Immunohistochemistry

Tissues were immersed in Tissue-Tek OCT (Bayer) and quick-frozen on dry ice. Using cryomicrotome and sialin-coated SuperFrost Plus slides (Fisher Scientific), 6- $\mu$ m tissue sections were cut. Sections were then fixed with 90% ethanol at -20°C, and after washing in PBS, an avidin/biotin-blocking step was included (Vector Laboratories). Primary and biotinylated secondary Abs (Vector Laboratories) were reacted with the sections for 60 min each, and color reaction was obtained by sequential incubation with avidin-peroxidase conjugate (Vector Laboratories) and diaminobenzidine-hydrogen peroxide. Primary Abs were rat anti-mouse CD8a (Ly2), rat anti-mouse CD4 (BD Pharmingen), and rat anti-mouse F4/80 (Serotec).

### Flow cytometry

For intracellular stains, single-cell suspensions were restimulated for 5 h with 1  $\mu$ g/ml MHC class I-restricted viral peptides in the presence of brefeldin A. Cells were stained for surface expression of CD4 and CD8, fixed, permeabilized, and stained for intracellular IFN- $\gamma$  (Abs were obtained from BD Pharmingen). Samples were acquired using a FACSCalibur (BD Biosciences).

### CTL assays

CTL activity for LCMV-specific responses was measured in a standard 5-h in vitro <sup>51</sup>Cr release assay using syngeneic (MC57, H-2<sup>b</sup>) target cells infected with LCMV (multiplicity of infection, 0.1) (23).

### Determination of viral titers by plaque assay

Viral titers of organ homogenates were determined by infection of Vero cells as previously described (23). Tissues (spleen, PDLN, and pancreas) were obtained from RIP-CXCL10 and wild-type C57BL/6J mice (three animals per group) on days 3 and 7 after infection with 10<sup>5</sup> LCMV i.p. Homogenates and sera were diluted serially, and viral titers were calculated from the number of counted plaques.

### In situ tetramer stains

Briefly, 6- $\mu$ m fresh-frozen sections were cut from the organs of interest and stained with a PE-labeled MHC class I tetramer (1.0  $\mu$ g/ml) with 2%

normal goat serum (NGS) and rat anti-CD8 $\alpha$  Ab (0.5  $\mu$ g/ml). Staining with tetramer containing an irrelevant peptide was used as a negative control. After an overnight incubation at 4°C, sections were washed in PBS and then fixed for 30 min at room temperature with PBS-buffered 2% formaldehyde. Sections were washed again in PBS and incubated for 3 h at 4°C with polyclonal rabbit anti-PE diluted 1/2500 in PBS with 2% NGS. Afterward, sections were washed and incubated for 3 h at 4°C with a Rhodamine Red X-conjugated donkey anti-rabbit Ab and an FITC-conjugated goat anti-rat Ab diluted 1/1000 in PBS with 2% NGS. Rhodamine Red X-positive and CD8-FITC-positive T lymphocytes were analyzed using a confocal microscope (21).

## Results

### Generation of RIP-CXCL10 transgenic mice

RIP-CXCL10 transgenic mice were generated by standard microinjection of C57BL/6J fertilized eggs with a construct containing mouse CXCL10, cloned from LPS-stimulated B10.D2 (C57BL/10 congenic) fibroblast cDNA (Fig. 1A). Transgene expression was controlled by the rat insulin II promoter, and transgenic mice were identified by PCR using an RIP-specific 5' primer and a CXCL10-specific 3' primer (Fig. 1B). The use of C57BL/10 CXCL10 cDNA facilitated detection of transgene-derived chemokine expression independent of endogenous chemokines due to a polymorphism in the CXCL10 gene. In RNase protection assays, bands of two different sizes could be detected using the mCK-5 multiprobe set (BD Pharmingen) depending on the mouse strain (24). Expression of the shorter transgenic CXCL10 product was easily distinguished from that of the longer endogenous C57BL/6 variant (Fig. 1C). We found that transgenic CXCL10 mRNA was predominantly expressed in the pancreas of RIP-CXCL10 transgenic mice. In contrast, no expression was detected in littermates (Fig. 1C) that tested negative for transgenic CXCL10 integration by PCR. Furthermore, immunofluorescent staining of tissue sections revealed that RIP-CXCL10 mice express CXCL10 protein in the pancreas. CXCL10 protein colocalized with insulin, indicating specific expression by  $\beta$  cells (Fig. 1D). Expression of CXCL10 in the islets was detected as early as day 2 after birth (data not shown). No CXCL10 expression was found in age-matched nontransgenic littermates (Fig. 1D).

### RIP-CXCL10 mice have spontaneous islet infiltration and impaired $\beta$ cell function, but do not develop spontaneous diabetes

Islet-specific expression of CXCL10 resulted in spontaneous infiltration of mononuclear cells into the pancreas. Most islets of RIP-CXCL10 mice displayed massive peri-insular infiltration composed predominantly of CD8 and CD4 T cells. Interestingly, intraislet infiltration by some CD8 and CD4 T cells was detected as well. In contrast, no T cells could be detected in age-matched nontransgenic littermates (Fig. 2A). The finding constitutes a proof-of-principle that potentially autoaggressive T cells can travel toward a high local gradient of CXCL10.

The presence of such a high number of T cells in and around the islets resulted in impaired  $\beta$  cell function, as revealed by glucose tolerance experiments. Mice were administered a high dose of glucose (i.p. injection of 1.5 mg/g body weight glucose), and the ability to regulate the blood glucose level to normoglycemia was assessed over time. After 10 min of glucose injection, blood glucose was increased to values ~300 mg/dl in both RIP-CXCL10 mice and nontransgenic littermates (Fig. 2B). Thereafter, blood glucose levels rapidly declined, with an approximate half-life of 30 min in wild-type mice. In contrast, RIP-CXCL10 mice had an impaired ability to down-regulate their blood glucose. After a stable phase of high blood glucose, the values started to decline only after 40 min, and the approximate half-time to return to levels



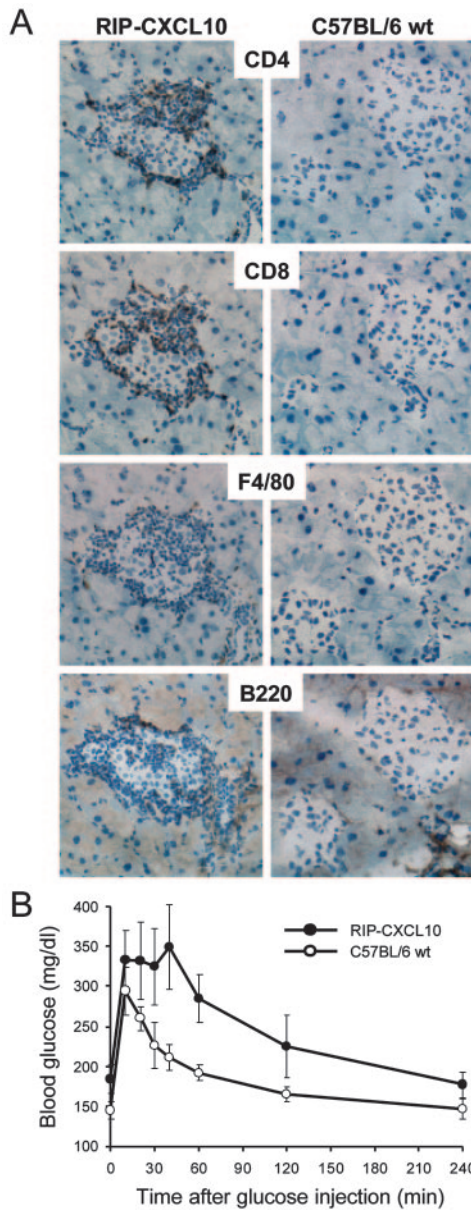


**FIGURE 2.** RIP-CXCL10 mice have spontaneous insulinitis. *A*, Pancreata were harvested from 4-wk-old RIP-CXCL10 mice or nontransgenic littermates (C57BL/6), and tissue sections were stained for the presence of CD4 and CD8 T cells, B cells (B220), and macrophages (F4/80). Note the massive peri- and intraislet infiltration in mice expressing CXCL10 in the islets. *B*, Glucose tolerance assay. Groups of five RIP-CXCL10 mice (●) or nontransgenic littermates (C57BL/6 wt; ○) were challenged with a single i.p. injection of 1.5 mg/g body weight glucose, and blood glucose values were measured over time as indicated.

similar to those before the challenge was 100 min (Fig. 2*B*). Similar data were obtained when RIP-CXCL10 mice were crossed to RIP-NP mice (data not shown). These data indicate that the presence of unspecific bystander T cells in the islets of Langerhans impairs the function of  $\beta$  cells under extreme conditions, such as high glucose challenge.

Despite the observed impairment of  $\beta$  cell function under stress conditions, none of the RIP-CXCL10 mice developed spontaneous T1D during the observation time (blood glucose <200 mg/dl for up to 6 mo of age; data not shown). Our data indicate that CXCL10 directs CD8 and CD4 T cells to the islets of Langerhans. This bystander inflammation of the pancreas is sufficient to induce lim-

ited  $\beta$  cell impairment, but is insufficient to cause islet destruction to the extent necessary for inducing clinically overt autoimmune disease.

*Constitutive pancreatic CXCL10 expression does not change LCMV clearance*

Despite greater influx of lymphocytes into the pancreas, the clearance of LCMV did not significantly change in RIP-CXCL10 mice after infection with  $10^5$  PFU of LCMV. Viral plaque assays revealed a similar viral titer in pancreas, PDLN, and spleen of RIP-CXCL10 and wild-type C57BL/6 mice on days 3 and 7 after LCMV infection (Fig. 3*A*).

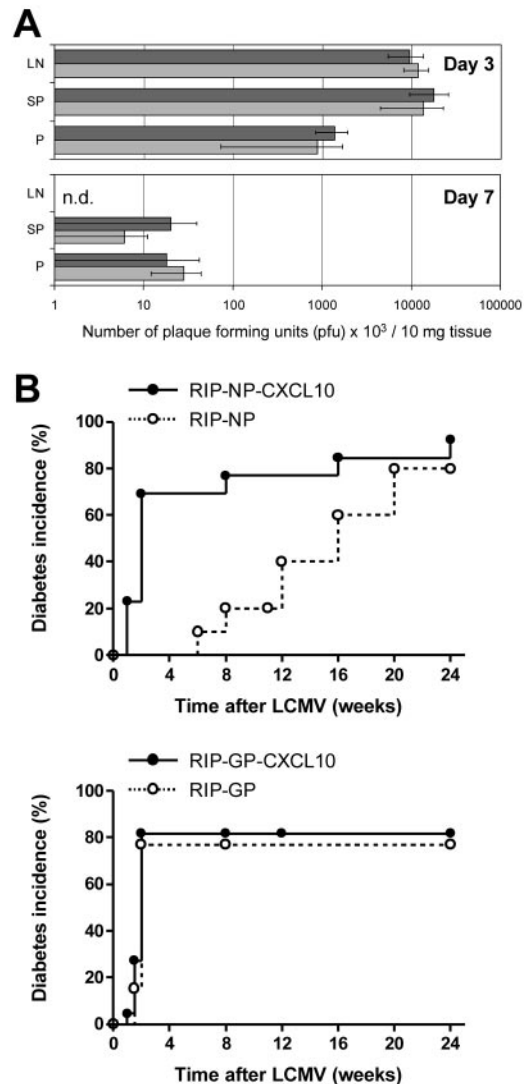


**FIGURE 3.** Islet-specific CXCL10 expression accelerates virus-induced diabetes. *A*, Expression of transgenic IP-10 in the pancreas had no effect on the kinetics of LCMV clearance after infection. Virus titers in the PDLN (LN), spleen (SP), and pancreas (P) on days 3 and 7 after infection are displayed. Data are the mean  $\pm$  SD of five mice per group. n.d., no plaques detectable at highest tissue homogenate concentration. *B*, RIP-LCMV-CXCL10 mice were infected with LCMV, and blood glucose was measured at weekly intervals (values >300 mg/dl were considered diabetic). Note that the development of T1D is significantly accelerated in RIP-NP-CXCL10 double-transgenic mice compared with single-transgenic RIP-NP mice (upper panel). CXCL10 expression did not further accelerate T1D in the fast-onset RIP-GP line (lower panel).

### Islet-specific CXCL10 expression accelerates virus-induced diabetes

To examine the influence of constitutive  $\beta$  cell CXCL10 expression on the kinetics of T1D development, we crossed RIP-CXCL10 mice with RIP-GP (fast-onset diabetes) and RIP-NP (slow-onset diabetes) transgenic mice. We found that  $\beta$  cell-specific expression of CXCL10 induced marked acceleration of LCMV-induced T1D in the slow-onset RIP-NP line (Fig. 3B). The kinetics of T1D development in these RIP-NP-CXCL10 double-transgenic mice were similar to those of the fast-onset disease observed among RIP-GP mice, where most animals became diabetic within 2 wk of LCMV infection (Fig. 3B). In contrast, no significant change in disease kinetics could be detected in the RIP-GP-CXCL10 double-transgenic mice compared with RIP-GP control mice (Fig. 3B). Thus, it appears that CXCL10 expression promotes marked disease acceleration, except in model systems where disease onset is already very rapid.

Consistent with the swift rise in blood glucose levels, constitutive CXCL10 expression promoted relatively rapid accumulation of CD8 cells in islet tissue of RIP-NP-CXCL10 mice. Four weeks after LCMV infection, no infiltration was evident in pancreatic tissue of RIP-NP mice, and insulin production was intact, as determined by immunohistochemistry (Fig. 4, upper panel). In contrast, at the same time both the single-transgenic RIP-CXCL10 mice and RIP-NP-CXCL10 mice had massive intraislet infiltrations by CD8 T cells (Fig. 4, middle and lower panels). Notably, RIP-CXCL10 mice had functional  $\beta$  cells, as indicated by intact insulin production (Fig. 4, middle panel), whereas insulin production was nearly absent in RIP-NP-CXCL10 mice, with only a few functional  $\beta$  cells remaining (Fig. 4, lower panel).

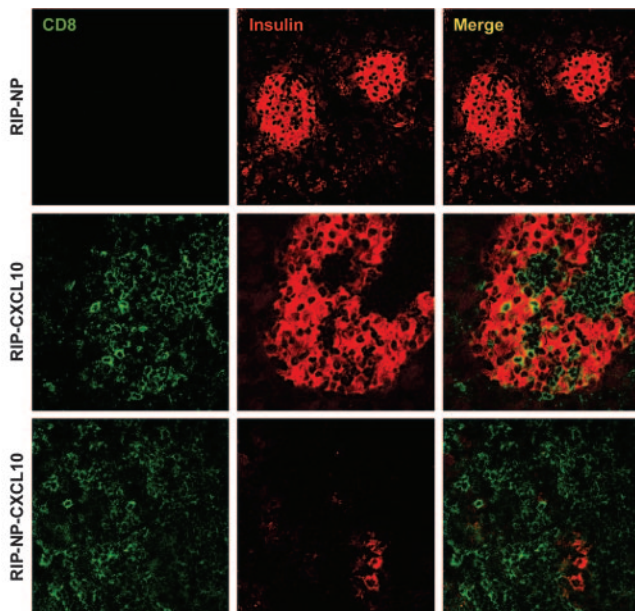


**FIGURE 4.** Acceleration of diabetes is reflected by enhanced insulinitis and impaired insulin production. Immunohistochemical examination of pancreata of RIP-NP, RIP-CXCL10, and RIP-NP-CXCL10 mice for CD8 T cell infiltration (green) and insulin production (red) at wk 4 after infection with LCMV. Note that RIP-CXCL10 and RIP-NP-CXCL10 mice showed a similar degree CD8 T cell infiltration. However, only diabetic RIP-LVMV-NP-CXCL10 double-transgenic mice abrogated  $\beta$  cell function, as characterized by impaired insulin expression.

### Ag-specific T cell migration to the pancreas was enhanced in RIP-CXCL10 mice

Next, we analyzed the quantity and functional activity of Ag-specific CD8 T cells in RIP-NP-CXCL10 and single-transgenic RIP-NP mice on days 5 and 8 after LCMV infection. H-2D<sup>b</sup>(LCMV-peptide) tetramers were used to detect CD8 T cells specific for the immunodominant LCMV-NP or LCMV-GP epitopes, NP396–404 (NP<sub>396</sub>) or gp33–41 (GP<sub>33</sub>), respectively. Staining with H-2Db(NP<sub>396</sub>) tetramers revealed a significantly reduced frequency of NP<sub>396</sub>-specific CD8 T cells in the spleens of RIP-NP-CXCL10 mice on day 8 after LCMV infection compared with RIP-NP mice (Fig. 5A). This reduction was associated with a decreased frequency of CD8 T cells that produced IFN- $\gamma$  upon stimulation with NP<sub>396</sub> peptide (Fig. 5B). In contrast, no reduction could be observed for GP<sub>33</sub>-specific CD8 T cells, whose target Ag is not in the pancreas (Fig. 5A). There was even an increased number of CD8 T cells that showed functional activity in the intracellular cytokine-staining assay (ICCS) for IFN- $\gamma$  (Fig. 5B). No significant differences in tetramer staining and ICCS for NP<sub>396</sub> and GP<sub>33</sub> between RIP-NP and RIP-NP-CXCL10 mice was detected on day 5 after LCMV infection (Fig. 5A).

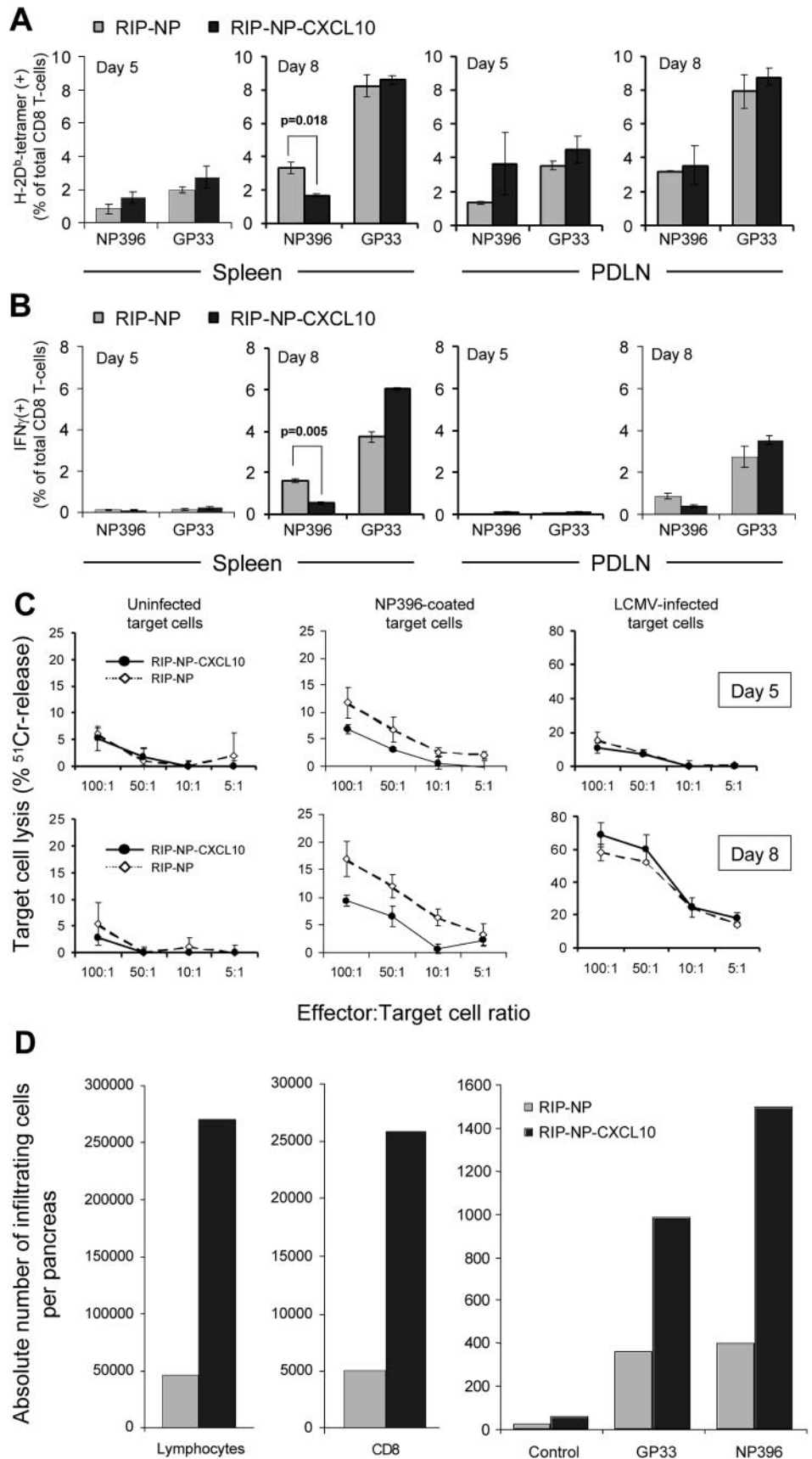
A similar outcome was observed in cytotoxicity <sup>51</sup>Cr release assays (CTL assay). Target cells were either infected with LCMV or coated with NP<sub>396</sub> peptide and incubated at different E:T cell ratios with splenocytes from RIP-NP or RIP-NP-CXCL10 mice isolated 5 or 8 days after LCMV infection. Lytic activity of splenocytes to NP<sub>396</sub>-coated target cells was reduced in splenocytes of RIP-NP-CXCL10 mice compared with RIP-NP splenocytes (Fig. 5C). In contrast, no significant change in lytic activity was detected against LCMV-infected target cells, which present all the viral GP and NP epitopes (Fig. 5C). In summary, the data obtained from tetramer staining, ICCS, and CTL assays demonstrate that the frequency of CD8 T cells with specificity to the pancreatic target Ag (NP) is reduced in the spleens of mice that express CXCL10 in the pancreas.

The obvious conclusion would be that NP-specific cells migrate to and remain in the pancreas, where both a high CXCL10 concentration and the target Ag are located. Indeed, isolation of lymphocytes directly from the pancreas on day 8 after infection with LCMV revealed a much greater number of NP<sub>396</sub>-specific CD8 T cells in the pancreas of RIP-NP-CXCL10 mice (Fig. 5D). As expected from our initial immunohistological studies (Fig. 2), the total number of lymphocytes and, in particular, CD8 T cells was enhanced in mice that expressed CXCL10 (Fig. 5D, left and middle panels). LCMV-specific cells (GP<sub>33</sub> and NP<sub>396</sub>) were detected in both RIP-NP and RIP-NP-CXCL10 mice. This is not unexpected, because the pancreas itself is infected by LCMV. However, the number of NP<sub>396</sub>-specific CD8 T cells is strikingly elevated in mice expressing CXCL10 in the islets (Fig. 5D, right panel). A higher frequency of GP<sub>33</sub>-specific CD8 T cells was noted as well. Together with the overall increase in CD8 T cell frequency, these data indicate an enhanced influx of nonspecific bystander cells into the pancreas.

### Islet-specific CXCL10 expression causes Ag-specific T cells to remain in the islets after LCMV infection

Next, we asked whether autoaggressive CD8 T cells, after being attracted by CXCL10, remained in the islets of Langerhans. Thus, we performed in situ staining on frozen pancreas sections similar to our previous reports for GP<sub>33</sub>-specific CD8 T cells in the CNS (21) and NP<sub>205</sub>-specific CD8 T cells in the islets of Langerhans (25). Dual staining with H-2D<sup>b</sup>-NP<sub>396</sub> tetramers and anti-CD8 Ab revealed that 4 wk after LCMV infection, NP<sub>396</sub>-specific CD8 T

**FIGURE 5.** The antiviral (self) immune response is decreased in the spleen, but increased in the pancreas of CXCL10-expressing mice. *A*, Flow cytometry and H-2D<sup>b</sup>(NP<sub>396</sub>) and H-2D<sup>b</sup>(GP<sub>33</sub>) tetramers were used to assess the frequency of LCMV-specific CD8 T cells on days 5 and 8 after LCMV infection in the spleen and PDLN of RIP-NP or RIP-NP-CXCL10 mice. Data are the mean ± SEM of three or four mice per group. Significant differences, analyzed using Student's *t* test, are displayed. *B*, The functional activity of LCMV-specific CD8 T cells on days 5 and 8 after LCMV infection in the spleen and PDLN of RIP-NP or RIP-NP-CXCL10 mice was analyzed by intracellular cytokine staining (IFN-γ) after 5-h in vitro stimulation with NP<sub>396</sub> or GP<sub>33</sub> peptide. Data are the mean ± SEM of three or four mice per group. Significant differences, analyzed using Student's *t* test, are displayed. *C*, Specific cytotoxicity of target cells by splenocytes isolated on days 5 and 8 after LCMV infection from RIP-NP or RIP-NP-CXCL10 mice (CTL assay). <sup>51</sup>Cr release was determined after a 5-h incubation of splenocytes (effector cells) with C57BL/6 fibroblasts that were infected with LCMV or coated with NP<sub>396</sub> (target cells) at several E:T cell ratios. *D*, The absolute numbers of lymphocytes, CD8 T cells, and functional NP<sub>396</sub>- and GP<sub>33</sub>-specific T cells in the pancreas on day 8 after LCMV infection were determined by flow cytometry after intracellular cytokine staining for IFN-γ after a 5-h stimulation with NP<sub>396</sub> or GP<sub>33</sub>. Cells from three pancreata of either RIP-NP or RIP-NP-CXCL10 mice were pooled. The entire cell suspension was acquired by flow cytometry to provide the total number of infiltrating cells.





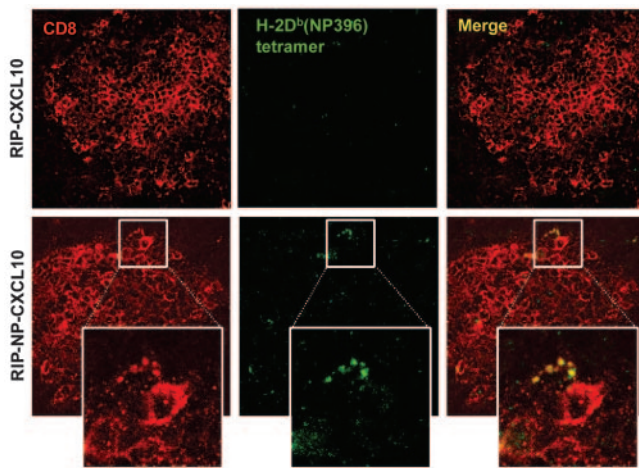


**FIGURE 6.** In situ tetramer staining of pancreas sections. Pancreata were harvested at wk 4 after LCMV infection. Tissue sections were cut and stained with anti-CD8 Abs (red) and H-2D<sup>b</sup>(NP<sub>396</sub>) tetramers (green). Between one and three NP<sub>396</sub>-specific CD8 T cells could be found in ~50% of islets in double-transgenic RIP-NP-CXCL10 mice. Note the characteristic clustering of H-2D<sup>b</sup>(NP<sub>396</sub>) tetramers (*lower panel, magnified inset*), indicating TCR aggregation and the formation of an immunologic synapse, as described for a similar LCMV-peptide tetramer H-2D<sup>b</sup>(GP<sub>33</sub>) in the brain after intracranial infection with LCMV (21).

cells were present exclusively in islets of RIP-NP-CXCL10 mice (Fig. 6). Between one and three NP<sub>396</sub>-specific CD8 T cells were found in ~50% of all islet sections analyzed. Quantification of our data indicated that ~2–3% of all infiltrating CD8 T cells are NP<sub>396</sub> specific in LCMV-infected RIP-NP-CXCL10 mice. This is consistent with the frequencies found in the PDLN, as determined by flow cytometry (Fig. 5A). In contrast, none of the islet sections examined from LCMV-infected RIP-CXCL10 mice (Fig. 6) had any NP<sub>396</sub>-specific CD8 T cells in the islets. Likewise, no NP<sub>396</sub>-specific CD8 T cells were found in pancreatic tissue from RIP-NP mice (data not shown), which do not exhibit insulinitis at 4 wk after infection.

## Discussion

In this paper we report three novel findings discovered in a newly generated transgenic mouse that expresses the CXCR3 chemokine ligand CXCL10 (IP-10) specifically in the  $\beta$  cells of pancreatic islets of Langerhans. First,  $\beta$  cell-specific expression of CXCL10 causes infiltration of lymphocytes into the islets of Langerhans, which causes limited impairment of  $\beta$  cell function under stress conditions. However, expression of transgenic CXCL10 in the islets is not sufficient to break the tolerance of peripheral lymphocytes with potential autoreactivity to islet Ags, as indicated by the lack of development of spontaneous diabetes. Second,  $\beta$  cell-specific CXCL10 expression causes massive acceleration of virus-induced T1D in RIP-LCMV-NP mice. Third, at an early time after infection, islet Ag-specific CD8 T cells were retained only in RIP-LCMV mice that expressed CXCL10.

RIP-CXCL10 mice were generated in a pure C57BL/6 background using *crq-2* (mouse homologue of CXCL10) cDNA obtained from a C57BL/10 fibroblast cell line and RIP to ensure  $\beta$  cell-specific expression. The inherent polymorphism in CXCL10 between those two mouse strains (24) allowed us to use RPA to characterize the expression of transgenic CXCL10 in different organs of RIP-CXCL10 mice and to distinguish transgenic from endogenous CXCL10. Transgenic CXCL10 mRNA was predominantly found in the pancreas, and immunofluorescence studies

revealed the expression of CXCL10 protein in the islets of Langerhans that colocalized with insulin, indicating  $\beta$  cell-specific expression of CXCL10 in RIP-CXCL10 mice. As a consequence of  $\beta$  cell-specific expression of CXCL10, islets were infiltrated by mononuclear cells. Infiltration was peri- and intrainsular and consisted predominantly of CD4 and CD8 T cells. Interestingly, the T cells were not prevented from entering the islets, similar to observations in NOD mice at an early prediabetic stage (26). This finding stands in contrast with data from other studies using transgenic mice expressing proinflammatory factors in the  $\beta$  cells, such as the RIP-IL-12 transgenic mouse, in which infiltration of mononuclear cells occurs only in a peri-insular fashion (27). As with  $\beta$  cell-specific expression of IL-12 (27) or TNF- $\alpha$  (28), CXCL10 expression did not break peripheral tolerance to islet Ags, and diabetes did not develop spontaneously. When these single-transgenic mice were crossed with RIP-LCMV mice that express the viral target Ag GP or NP, the resulting double-transgenic RIP-NP-CXCL10 and RIP-GP-CXCL10 mice had infiltrations similar to those of single-transgenic RIP-CXCL10 mice. Again, there was no development of spontaneous T1D in either of these double-transgenic mouse lines.

Although CXCL10-induced bystander inflammation was insufficient to cause overt autoimmune disease, a limited effect on  $\beta$  cell function was detected under stress conditions. RIP-CXCL10 mice were not able to efficiently down-regulate blood glucose levels after a high glucose challenge experiment. It was previously demonstrated in another experimental setup that bystander inflammation alone is sufficient to induce T1D (29). Infection of mice with a TCR transgene specific for an islet autoantigen with coxsackie B4 virus results in the rapid development of T1D (29). However, although coxsackie B4 virus infection was suggested to cause tissue destruction and release of sequestered islet Ag, which activates resting autoaggressive T cells, CXCL10 seems to cause attraction, rather than activation, of T cells.

Although no spontaneous T1D developed in RIP-CXCL10 mice,  $\beta$  cell-specific CXCL10 expression massively accelerated a pre-existing autoimmune condition. The majority of RIP-NP-CXCL10 mice developed T1D within 2 wk of infection with LCMV, whereas the onset of T1D in single-transgenic RIP-NP mice ranged from 1 to 5 mo. Acceleration of virus-induced T1D in RIP-NP-CXCL10 mice was reflected in the abrogation of functional activity of islets at an early stage (wk 4) after LCMV infection. At the same time, RIP-NP single-transgenic mice showed negligible infiltrations and totally functional  $\beta$  cells. No significant acceleration could be observed in RIP-GP-CXCL10 mice. Because of the presence of high affinity, autoaggressive CD8 T cells, regular RIP-GP mice develop T1D, independent of CD4 T cells, very rapidly after LCMV infection (20). Constitutive CXCL10 expression is unable to further accelerate immunopathological damage to the islets and the resulting onset of hyperglycemia in this model. These findings are in agreement with studies performed with RIP-LCMV-IL-12 mice, in which acceleration of disease was only observed in RIP-NP-IL-12 mice (27). In contrast to other transgenic mouse models that use transgenic technique to express proinflammatory factors in the islets, RIP-CXCL10 mice express a chemoattractant factor that by itself directly causes infiltration into the islets. It is very likely that islet infiltrations observed in RIP-IFN- $\gamma$  (30, 31), RIP-TNF- $\alpha$  (28), and RIP-IL-12 (27) mice are caused by induction of chemokine expression by the individual transgenically expressed cytokines that, in turn, recruits lymphocytes to the islets. CXCL10 is a likely candidate to be involved in such a mechanism, because its expression is induced by both IFN- $\gamma$  and TNF- $\alpha$  (4, 5).

Islet-specific expression of CXCL10 impacts the anti-LCMV immune response by recruiting LCMV-specific CD8 T cells from the systemic lymphocyte pool to the pancreas. Both the frequency and the overall antiviral functional activity were reduced in the spleens of RIP-NP-CXCL10 mice compared with RIP-NP mice. However, no changes in viral clearance were noted, indicating that the immune response is still sufficient to control virus growth and elimination. At the same time, the total number of CD8 T cells in the pancreas was massively increased in RIP-NP-CXCL10 mice, which is in agreement with immunohistochemical analysis showing insulinitis. Assessment of the functional activity of islet Ag (NP)-specific CD8 T cells by ICCS revealed that up to 4 times more NP-specific CD8 T cells are present in the pancreas of RIP-NP-CXCL10 mice than in RIP-NP mice. When focusing on their actual presence in the islets of Langerhans, we found, by in situ tetramer staining, that at an early stage after infection, NP<sub>396</sub>-specific CD8 T cells were only present in RIP-NP-CXCL10 mice, not in RIP-NP mice. RIP-NP mice do not have significant infiltrations at that time, whereas RIP-CXCL10 transgenic mice do, but neither develops overt diabetes.

In summary, our data indicate that bystander inflammation of the pancreas of uninfected RIP-CXCL10 mice caused by  $\beta$  cell-specific CXCL10 expression does result in a functional impairment of  $\beta$  cells, but is not sufficient by itself to induce autoimmunity. This functional impairment seems to be caused by the presence of large numbers of unspecific bystander cells. We found that such islet infiltrates predominantly consisted of CD8 and CD4 T cells and, to lesser a degree, B cells and macrophages. Thus, the question arises of how those Ag-nonspecific cells contribute to the observed acceleration of T1D once mice have been infected with LCMV. Previous studies demonstrated that neither B cells nor LCMV-specific Abs are required to precipitate disease in the RIP-LCMV model (32). However, in contrast to RIP-LCMV-GP mice, which develop fast-onset T1D without CD4 T cell help, RIP-LCMV-NP mice require the presence of functional Ag-specific CD4 T cells (20). In addition, we found in an earlier study that the T cell chemokine CCL5 (RANTES) and the proinflammatory cytokines TNF- $\alpha$  and IFN- $\gamma$  are extensively up-regulated in the pancreas at the time of T cell infiltration (2). Blocking of CCL5 during its peak of pancreatic expression neither reduced the frequency of T1D nor changed the overall kinetics of disease onset (2). In contrast, neutralization of CXCL10 massively reduced T1D by blocking the expansion and migration of LCMV-specific CD8 T cells to the pancreas (2). Blocking of CXCL10 was successful for two major reasons: 1) 95% of LCMV-specific CD8 T cells express the cellular receptor for CXCL10, CXCR3, after infection with LCMV; and 2) CXCL10 is massively and uniquely expressed very early after LCMV infection (2). Concluding from those previous (2) and present data, the presence of a sufficient number of islet-specific lymphocytes is an absolute prerequisite for the auto-aggressive destruction of  $\beta$  cells and the subsequent development of diabetes. This conclusion is supported by our recent observation that molecular mimicry of an islet Ag by an infecting virus is not enough to induce autoimmune disease when the frequency of islet-specific CD8 T cells after infection does not exceed a minimum threshold for sufficient  $\beta$  cell destruction (25). However, just like islet-specific expression of CXCL10 or IL-12 (27), which both accelerated the influx of autoaggressive cells into the pancreas, molecular mimicry by a second infecting virus enhanced the numbers of Ag-specific antiviral (self) T cells to the level required to accelerate a pre-existing autoimmune condition (25). Our data are proof-of-principle that enhanced local inflammation accelerates the general migration of lymphocytes to their target site. However, treatment of human individuals suffering from T1D with anti-

chemokine (e.g., CXCL10) Abs is problematical, because the events that might have caused a CXCL10 burst occurred early after infection, long before T1D clinical manifestation. In contrast, administration of anti-chemokine Abs after defined events that lead to high local inflammation, such as the transfusion of purified islets of Langerhans (33), should be clinically feasible, because islet transfusion and anti-CXCL10 Ab treatment can be timed appropriately.

## Disclosures

The authors have no financial conflict of interest.

## References

- Frigerio, S., T. Junt, B. Lu, C. Gerard, U. Zumsteg, G. A. Hollander, and L. Piali. 2002.  $\beta$  cells are responsible for CXCR3-mediated T-cell infiltration in insulinitis. *Nat. Med.* 8: 1414–1420.
- Christen, U., D. B. McGavern, A. D. Luster, M. G. von Herrath, and M. B. Oldstone. 2003. Among CXCR3 chemokines, IFN- $\gamma$ -inducible protein of 10 kDa (CXC chemokine ligand (CXCL) 10) but not monokine induced by IFN- $\gamma$  (CXCL9) imprints a pattern for the subsequent development of autoimmune disease. *J. Immunol.* 171: 6838–6845.
- Narumi, S., T. Kaburaki, H. Yoneyama, H. Iwamura, Y. Kobayashi, and K. Matsushima. 2002. Neutralization of IFN-inducible protein 10/CXCL10 exacerbates experimental autoimmune encephalomyelitis. *Eur. J. Immunol.* 32: 1784–1791.
- Luster, A. D., J. C. Unkeless, and J. V. Ravetch. 1985.  $\gamma$ -Interferon transcriptionally regulates an early-response gene containing homology to platelet proteins. *Nature* 315: 672–676.
- Luster, A. D., and J. V. Ravetch. 1987. Biochemical characterization of a  $\gamma$  interferon-inducible cytokine (IP-10). *J. Exp. Med.* 166: 1084–1097.
- Gattass, C. R., L. B. King, A. D. Luster, and J. D. Ashwell. 1994. Constitutive expression of interferon  $\gamma$ -inducible protein 10 in lymphoid organs and inducible expression in T cells and thymocytes. *J. Exp. Med.* 179: 1373–1378.
- Liu, M. T., B. P. Chen, P. Oertel, M. J. Buchmeier, D. Armstrong, T. A. Hamilton, and T. E. Lane. 2000. The T cell chemoattractant IFN-inducible protein 10 is essential in host defense against viral-induced neurologic disease. *J. Immunol.* 165: 2327–2330.
- Kolb, S. A., B. Sporer, F. Lahrtz, U. Koedel, H. W. Pfister, and A. Fontana. 1999. Identification of a T cell chemotactic factor in the cerebrospinal fluid of HIV-1-infected individuals as interferon- $\gamma$  inducible protein 10. *J. Neuroimmunol.* 93: 172–181.
- Charles, P. C., X. Chen, M. S. Horwitz, and C. F. Brosnan. 1999. Differential chemokine induction by the mouse adenovirus type-1 in the central nervous system of susceptible and resistant strains of mice. *J. Neurovirol.* 5: 55–64.
- Asensio, V. C., and I. L. Campbell. 1997. Chemokine gene expression in the brains of mice with lymphocytic choriomeningitis. *J. Virol.* 71: 7832–7840.
- Hoffman, L. M., B. T. Fife, W. S. Begolka, S. D. Miller, and W. J. Karpus. 1999. Central nervous system chemokine expression during Theiler's virus-induced demyelinating disease. *J. Neurovirol.* 5: 635–642.
- Lane, T. E., V. C. Asensio, N. Yu, A. D. Paoletti, I. L. Campbell, and M. J. Buchmeier. 1998. Dynamic regulation of  $\alpha$ - and  $\beta$ -chemokine expression in the central nervous system during mouse hepatitis virus-induced demyelinating disease. *J. Immunol.* 160: 970–978.
- Khan, I. A., J. A. MacLean, F. S. Lee, L. Casciotti, E. DeHaan, J. D. Schwartzman, and A. D. Luster. 2000. IP-10 is critical for effector T cell trafficking and host survival in *Toxoplasma gondii* infection. *Immunity* 12: 483–494.
- Luster, A. D., R. D. Cardiff, J. A. MacLean, K. Crowe, and R. D. Granstein. 1998. Delayed wound healing and disorganized neovascularization in transgenic mice expressing the IP-10 chemokine. *Proc. Assoc. Am. Physicians* 110: 183–196.
- Sallusto, F., A. Lanzavecchia, and C. R. Mackay. 1998. Chemokines and chemokine receptors in T-cell priming and Th1/Th2-mediated responses. *Immunol. Today* 19: 568–574.
- Loetscher, M., B. Gerber, P. Loetscher, S. A. Jones, L. Piali, I. Clark-Lewis, M. Baggiolini, and B. Moser. 1996. Chemokine receptor specific for IP10 and Mig: Structure, function, and expression in activated lymphocytes. *J. Exp. Med.* 184: 963–969.
- Morimoto, J., H. Yoneyama, A. Shimada, T. Shigihara, S. Yamada, Y. Oikawa, K. Matsushima, T. Saruta, and S. Narumi. 2004. CXC chemokine ligand 10 neutralization suppresses the occurrence of diabetes in nonobese diabetic mice through enhanced  $\beta$  cell proliferation without affecting insulinitis. *J. Immunol.* 173: 7017–7024.
- Christen, U., D. Benke, T. Wolfe, E. Rodrigo, A. Rhode, A. C. Hughes, M. B. Oldstone, and M. G. Von Herrath. 2004. Cure of prediabetic mice by viral infections involves lymphocyte recruitment along an IP-10 gradient. *J. Clin. Invest.* 113: 74–84.
- Oldstone, M. B. A., M. Nerenberg, P. Southern, J. Price, and H. Lewicki. 1991. Virus infection triggers insulin-dependent diabetes mellitus in a transgenic model: role of anti-self (virus) immune response. *Cell* 65: 319–331.
- von Herrath, M. G., J. Dockter, and M. B. A. Oldstone. 1994. How virus induces a rapid or slow onset insulin-dependent diabetes mellitus in a transgenic model. *Immunity* 1: 231–242.



21. McGavern, D. B., U. Christen, and M. B. Oldstone. 2002. Molecular anatomy of antigen-specific CD8<sup>+</sup> T cell engagement and synapse formation in vivo. *Nat. Immunol.* 3: 918–925.
22. von Herrath, M. G., S. Guerder, H. Lewicki, R. A. Flavell, and M. B. Oldstone. 1995. Coexpression of B7-1 and viral (“self”) transgenes in pancreatic  $\beta$  cells can break peripheral ignorance and lead to spontaneous autoimmune diabetes. *Immunity* 3: 727–738.
23. von Herrath, M. G., J. Dockter, M. Nerenberg, J. E. Gairin, and M. B. A. Oldstone. 1994. Thymic selection and adaptability of cytotoxic T lymphocyte responses in transgenic mice expressing a viral protein in the thymus. *J. Exp. Med.* 180: 1901–1910.
24. Hallensleben, W., L. Biro, C. Sauder, J. Hausmann, V. C. Asensio, I. L. Campbell, and P. Staeheli. 2000. A polymorphism in the mouse *crg-2/IP-10* gene complicates chemokine gene expression analysis using a commercial ribonuclease protection assay. *J. Immunol. Methods* 234: 149–151.
25. Christen, U., K. H. Edelmann, D. B. McGavern, T. Wolfe, B. Coon, M. K. Teague, S. D. Miller, M. B. Oldstone, and M. G. von Herrath. 2004. A viral epitope that mimics a self antigen can accelerate but not initiate autoimmune diabetes. *J. Clin. Invest.* 114: 1290–1298.
26. Bach, J.-F. 1994. Insulin dependent diabetes mellitus as an autoimmune disease. *Endocr. Rev.* 15: 516–542.
27. Holz, A., K. Brett, and M. B. Oldstone. 2001. Constitutive  $\beta$  cell expression of IL-12 does not perturb self-tolerance but intensifies established autoimmune diabetes. *J. Clin. Invest.* 108: 1749–1758.
28. Picarella, D. E., A. Kratz, C. Li, N. Ruddle, and R. A. Flavell. 1993. Transgenic tumour necrosis factor (TNF)- $\alpha$  production in pancreatic islets leads to insulinitis, not diabetes. *J. Immunol.* 150: 4136–4150.
29. Horwitz, M. S., L. M. Bradley, J. Harbertson, T. Krahl, J. Lee, and N. Sarvetnick. 1998. Diabetes induced by coxsackie virus: initiation by bystander damage and not molecular mimicry. *Nat. Med.* 4: 781–785.
30. Lee, M.-S., M. G. von Herrath, H. Reiser, M. B. A. Oldstone, and N. Sarvetnick. 1995. Sensitization to self antigens by in situ expression of interferon- $\gamma$ . *J. Clin. Invest.* 95: 486–492.
31. Sarvetnick, N., D. Liggitt, S. L. Pitts, S. E. Hansen, and T. A. Stewart. 1988. Insulin-dependent diabetes mellitus induced in transgenic mice by ectopic expression of class II MHC and interferon- $\gamma$ . *Cell* 52: 773–782.
32. Holz, A., T. Dyrberg, W. Hagopian, D. Homann, M. Herrath, and M. B. Oldstone. 2000. Neither B lymphocytes nor antibodies directed against self antigens of the islets of Langerhans are required for development of virus-induced autoimmune diabetes. *J. Immunol.* 165: 5945–5953.
33. Shapiro, A. M., J. R. Lakey, E. A. Ryan, G. S. Korbutt, E. Toth, G. L. Warnock, N. M. Kneteman, and R. V. Rajotte. 2000. Islet transplantation in seven patients with type 1 diabetes mellitus using a glucocorticoid-free immunosuppressive regimen. *N. Engl. J. Med.* 343: 230–238.